THE ASTROPHYSICAL JOURNAL, 374:298–306, 1991 June 10

THE PULSE-TIMING AND EMISSION-LINE ORBITS OF THE WHITE DWARF IN THE CATACLYSMIC VARIABLE AE AQUARII

EDWARD L. ROBINSON, ALLEN W. SHAFTER,[1] AND S. BALACHANDRAN[2]
McDonald Observatory and Department of Astronomy, The University of Texas at Austin, Austin, TX 78712
Received 1990 August 23; accepted 1990 November 29

ABSTRACT

The nova-like variable AE Aqr is a binary star with an orbital period of 9.88 hr, consisting of a K5 V star and a white dwarf. The white dwarf is magnetized, and it is accreting mass transferred from the K5 V star onto its two magnetic poles. The white dwarf rotates with a period of 33.08 s causing flashes of unequal strength every 16.5 s. The orbital motion of the white dwarf has been estimated from the radial velocity curve of the emission lines produced in the accreting gas around the white dwarf and from the times of arrival of the 33.08 s pulses. We have remeasured both the emission-line and the pulse-timing orbits of AE Aqr. From the emission-line orbit we derive an improved value for the orbital period, 0.4116580($\pm$2) days, and an improved value for the amplitude of the radial velocity variations, $K_{em} = 141 \pm 8$ km s^{-1}. Based on our new photometry, the revised ephemeris for the 16.5 s component of the 33 s modulation is T_{max} = BJED 2,445,171.999844($\pm$1) + 0.000191416425($\pm$1)E, and the semiamplitude of the pulse-timing orbit is 2.30 $\pm$ 0.07 s, which is equivalent to $K_{pulse} = 122 \pm 4$ km s^{-1}. We show that the pulse-timing orbit is distorted, probably by reprocessing of the pulses in the accreting gas, and cannot be used to estimate the orbit of the white dwarf reliably. The emission-line orbit appears to be unusually free of complications and is a better estimator of the orbit of the white dwarf. Adopting the spectroscopic orbital elements for AE Aqr, we find $M_K \sin^3 i = 0.54 \pm 0.05\ M_\odot$, $M_{wd} \sin^3 i = 0.62 \pm 0.05\ M_\odot$, and $q = M_{wd}/M_K = 1.13 \pm 0.06$. The orbital inclination lies between 63° and 70°.

Subject headings: stars: binaries — stars: dwarf novae — stars: individual (AE Aqr) — stars: white dwarfs

1. INTRODUCTION

The reliability of the dynamical masses of cataclysmic variables, by which we mean masses determined directly from orbital motions, is uncertain. The spectra of the white dwarfs in cataclysmic variables are rarely visible and probably never uncontaminated by emission from accreting gas. As a result, the radial velocity of the white dwarf cannot be measured directly from its spectrum. Instead, one measures the radial velocities of the emission lines produced in the accretion disk around the white dwarf and assumes that the emission-line orbit is the same as the white dwarf orbit. While this assumption may be justified for some systems, particularly if the velocities are measured from the wings of the emission lines, there is ample evidence that emission-line orbits of some cataclysmic variables are distorted. The most conclusive evidence is that the times of spectroscopic conjunction of the emission-line orbits can be different from times of conjunction measured by other methods, such as from eclipse timings or from the spectroscopic orbit of the late-type star that is the companion to the white dwarf. The emission-line orbit of EM Cyg, for example, is shifted by $\sim$20° in orbital phase from the orbit of its dK companion (Stover, Robinson, & Nather 1981). While the extent to which these distortions bias measurements of the masses is unknown, the worry has been that the errors could be large.

Observations of the bright ($V \sim$ 10.0–12.5 mag) nova-like variable AE Aqr have the potential to resolve some of these questions because the orbit of its white dwarf can be measured in two independent ways: from the radial velocity curve of the emission lines in its spectrum and from the arrival times of coherent pulsations in its light curve. Like all cataclysmic variables, AE Aqr has an orbital period that is short enough, 9.88 hr (Walker 1965), that the late-type star fills or nearly fills its Roche lobe and transfers mass to the white dwarf. The rate of mass transfer has been variously estimated to be 6×10^{-11} to $1.6 \times 10^{-10}\ M_\odot$ yr^{-1} (Lamb & Patterson 1985; Jameson, King, & Sherrington 1980). The spectrum of AE Aqr has a K5 V or K5 IV–V absorption-line component that comes from the late-type star in the system, and it has an emission-line component with lines of H, He I, and Ca II that comes from the accreting gas near the white dwarf (Crawford & Kraft 1956; Chincarini & Walker 1981b). It is usually assumed, by analogy to other cataclysmic variables, that the accreting gas forms an accretion disk around the white dwarf, but the direct evidence for the disk is poor. Although AE Aqr has a high orbital inclination, its emission lines do not, for example, show the double peaks usually produced by nearly edge-on disks (Horne & Marsh 1986). The accretion disk may be less well formed in AE Aqr than in other cataclysmic variables. According to Chincarini & Walker (1981b), the amplitude of the radial velocity curve of the K5 V star is $K_K = 160 \pm 1$ km s^{-1}, and the amplitude of the emission-line radial velocity curve is $K_{em} = 135 \pm 5$ km s^{-1}.

The light curve of AE Aqr has three remarkable features: large flares, highly coherent pulsations at 33.08 s, and quasi-periodic oscillations. The large flares can have amplitudes greater than 1 mag and last from 10 minutes to an hour or more (Zinner 1938; Henize 1949; van Paradijs, Kraakman, & van Amerongen 1989). During the flares the light curve shows flickering similar to the flickering seen in other cataclysmic

[1] Present address: Department of Astronomy, San Diego State University, San Diego, CA 92182.
[2] Present address: Institute of Astronomy, University of Hawaii, 2680 Woodlawn Drive, Honolulu, HI 96822.

variables, but between flares there are intervals of up to a few hours during which the flickering disappears and the light curve is nearly quiescent. The precise nature of the flares is uncertain but they are associated with the accretion process. Variable radio emission has been detected from AE Aqr, suggesting that the flares are magnetic flares in the disk, possibly related to the flares in Cyg X-3 (Bookbinder & Lamb 1987; Bastian, Dulk, & Chanmugam 1988).

The coherent periodic modulation at 33.08 s has two nearly equal peaks per cycle, and thus a power spectrum of the modulation has a stronger peak at the 16.5 s first harmonic period than at the 33.08 s fundamental period. The semiamplitude is typically 0.2%–0.3% but can be as large as 1% (Patterson 1979). The modulation is highly stable in period. The upper limit to the rate of change of the pulse period is $\dot{P} \leq 10^{-14}$ s s^{-1} (Patterson, Beuermann, & Africano 1988). The X-ray flux from AE Aqr is also pulsed, with a period near 33 s (Patterson et al. 1980). Because the 33.08 s modulation is so short and so highly coherent, and because the X-ray flux from AE Aqr is also pulsed with a period of 33 s, it is generally accepted that the modulation is caused by rotation of the white dwarf and that the white dwarf is magnetized and is accreting mass onto its two magnetic poles. At a rotation period of 33.08 s the two poles cause flashes every 16.5 s.

The quasi-periodic oscillations are present in the light curve only during flares (Patterson 1979). They have mean periods slightly longer than the coherent modulations at 33.08 and 16.5 s, and their amplitudes can be substantially larger than the amplitude of the coherent modulations. As a result, the quasi-periodic oscillations distort the coherent modulations or mask them altogether. The quasi-periodic oscillations are probably caused by an interaction between the rotating white dwarf and blobs or inhomogeneities in the accretion disk or accretion column.

The 33.08 s pulses can be used to measure the orbit of the white dwarf, and, if the pulses are not reprocessed anywhere else in the system, the delays in the pulse arrival times should give an unbiased measurement of the orbit. Patterson (1979) measured the pulse orbit, finding that the orbit was nearly circular and nearly 180° out of phase with the orbit of the K5 V star, thus suggesting that the pulse-timing orbit was not greatly distorted. The amplitude of the pulse-timing orbit was equivalent to a radial velocity amplitude of $K_{\rm pulse} = 127 \pm 5$ km s^{-1}.

Our interest in AE Aqr was engendered by the possibility that a more precise comparison of the pulse-timing orbit with the emission-line orbit would help identify the sources of systematic biases in both, and lead to a more reliable determination of the orbital motion of the white dwarf. We have, therefore, remeasured both the pulse-timing and the emission-line orbits of the white dwarf. We show that the emission-line orbit is much less distorted than the pulse-timing orbit, and that the emission-line orbit should be a good estimator of the white dwarf orbit.

2. OBSERVATIONAL DATA

The spectroscopic data were obtained with the coudé spectrograph of the 2.1 m Struve telescope at McDonald Observatory on nine nights in 1985 September and October. The spectra were obtained using a Reticon silicon diode array as the detector and covered roughly 280 Å centered on 6600 Å at a reciprocal dispersion of 0.15 Å per diode (Vogt, Tull, & Kelton 1978). The typical exposure time was 30 minutes. We acquired 27 usable spectra between September 4 and 9 (UTC) and another 15 spectra between September 24 and October 3 (UTC).

TABLE 1

PHOTOMETRIC OBSERVATIONS OF AE AQUARII

Run Number	Integration Time (s)	Telescope (m)	BJED Start 2,445,000.0+	Duration (s)
2679	3	2.1	139.80385	1569
2691	3	0.9	172.83967	10056
2692	5	0.9	173.80886	3855
2694	3	0.9	175.87071	7092
2697	3	0.9	176.90961	4560
2703	5	0.9	201.80740	6950
2711	3	0.9	204.77202	3822
2728	1	2.1	254.58468	1900
2730	1	2.1	256.57700	10324
2734	1	2.1	257.57850	4000
2735	1	2.1	257.63329	2890
2738	1	2.1	258.57741	10110
2741	1	2.1	260.57102	3690
S&H2	1	0.9	528.71722	10989
S&H3	1	0.9	528.84725	6800
S&H4	1	0.9	530.81026	10675
2824	1	0.8	586.65163	7013
2825	1	0.8	586.74930	11398
2826	1	0.8	587.62602	8773
2827	1	0.8	587.73096	12081
2828	1	0.8	588.62820	10147
2829	1	0.8	589.64288	18442

The photometric observations were obtained on the 0.8 m, 0.9 m, and 2.1 m telescopes at McDonald Observatory on 13 nights in 1982 and six nights in 1983. S. Sawyer and B. P. Hine obtained three more nights of photometry for us in 1983. All the observations were made with the standard McDonald Observatory two-channel photometer (Nather 1973) equipped with a blue-sensitive photomultiplier tube (an RCA 8850). To maximize the photon count rate, all the observations were made without filters. The individual integrations were 1, 3, or 5 s long, and a typical run (one night's observation) lasted 2–3 hr. The run numbers, integration times, telescopes used, and lengths of the individual runs are given in Table 1; the runs obtained by Sawyer and Hine have numbers S&H2, S&H3, and S&H4. Our data are similar to those shown by Patterson (1979) and Patterson et al. (1980); the reader can refer to those papers for examples of the light curve of AE Aqr.

We used the observatory clock for all timings. The clock is set to UTC using the time signals broadcast by WWV, and is maintained within a few milliseconds of true UTC. The UTC times were converted to ephemeris time (ET) using the offsets tabulated in the Astronomical Almanac, and then corrected to the barycenter of the solar system using the positions and velocities of the Earth relative to the barycenter of the solar system given in the Astronomical Almanac. The barycentric timings are accurate to better than 0.1 s.

3. EMISSION-LINE RADIAL VELOCITY ORBIT

3.1. *A Preliminary Orbital Period for the Emission Lines*

The only feature strong enough to measure in the wavelength region covered by our spectra was the Hα emission line. We determined preliminary radial velocities for the Hα emission line by convoluting the line profiles with a template consisting of two Gaussians whose widths were much narrower

than the width of the line (Shafter 1985; Shafter, Szkody, & Thorstensen 1986). The template was positioned so that one Gaussian was in the blue wing of Hα and the other was in the red wing. The wavelength of the template was adjusted by a Newton-Raphson iteration procedure until the fluxes through the two Gaussians were equal. The wavelength of the midpoint of the Gaussians was then taken as the velocity of the emission line.

We determined a preliminary orbital period for the emission lines using the Lomb-Scargle algorithm for calculating periodograms (Lomb 1976; Scargle 1982). We calculated the periodogram using both our velocities and the emission-line given by Joy (1954). Joy's velocities and our velocities were obtained more than 30 years apart, and, therefore, the periodogram had many aliases. One period, at 0.411658 days, was slightly favored, but not by enough to justify chosing it as the correct period, and we were forced to use the orbital period for the absorption lines to narrow the choice to just one alias.

The data set for the absorption-line orbital period consists of the velocities tabulated by Chincarini & Walker (1981a). We do not, however, use the orbital period found by Chincarini & Walker because they combined the emission-line and absorption-line velocities in their analysis. The emission-line velocities came from Joy (1954) and were sparser and of lower quality than the absorption-line velocities, which were obtained by Walker with the Lallemand electronographic camera. Their inclusion degraded the accuracy of the period. The orbital period has been redetermined by Feldt & Chincarini (1980) using only the absorption-line velocities. They found

$$T_0 = \mathrm{JD}_\odot\ 2{,}439{,}030.827(\pm 3) + 0.4116579E\ , \qquad (1)$$

where T_0 is the time of inferior spectroscopic conjunction of the K5 V star (K5 V star toward the observer). There was no evidence for any secular change in the orbital period. Since the period found by Feldt & Chincarini (1980) is free of aliases, and since it agrees with the most favored alias in our periodogram, we chose $P = 0.4116579$ days for the preliminary orbital period. This preliminary period is roughly consistent with the orbital period determined from photometry of the light curve, 0.4116560 ± 0.0000005 days (van Paradijs et al. 1989).

3.2. *Orbital Elements*

The spectra published by Walker (1965) and Chincarini & Walker (1981b) show that the higher members of the Balmer series have complex and highly variable line profiles. In addition to the broad component that is usually attributed to the accretion disk, there are components due to the gas stream between the stars and others that may be caused by inhomogeneities within the disk. There is also a narrow feature caused by chromospheric emission from the K5 V star. Figure 1 shows the Hα line of AE Aqr as a function of orbital phase. The 42 individual spectra have been co-added into 10 orbital phase bins to reduce noise in the profiles. The Hα line profile is broad, and, with the possible exception of the profile at orbital phase $\phi = 0.9$, it is single-peaked. The profile is obviously variable, but not by as much as the higher members of the Balmer series. There is no evidence for an S-wave in the profile.

The irregularities in the line profile complicate measurement of the radial velocity variations because they introduce phase-dependent asymmetries in the line profile. Because these asymmetries come from features near the outer edge of the accretion disk and from the secondary star, they are confined to low

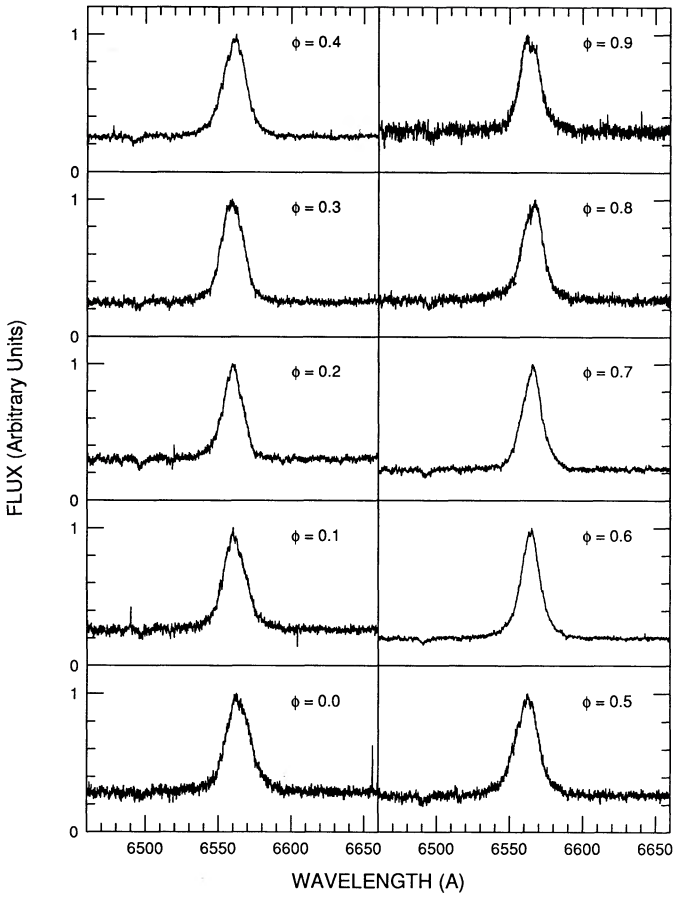

FIG. 1.—Hα emission line in AE Aqr as a function of orbital phase. The 42 individual spectra have been co-added into 10 orbital phase bins to reduce noise in the profiles. The profile of the Hα line is variable, but the largest variations appear to be concentrated toward the line center.

velocities and thus to regions near the center of the line profile. The line wings are formed near the center of the accretion disk where nonaxisymmetries in the accretion disk should be small, and they should be comparatively free of distortions. We have used the double-Gaussian method described in the previous section to measure the line wings. Since the line wings are noisy and may be contaminated by nearby emission lines, we have found it useful to measure radial velocities for a range of separations for the two Gaussians. With widely separated Gaussians the velocities are measured in the extreme line wings, and with small separations the velocities are measured nearer to the line center. Orbital solutions based on velocity measurements for a given Gaussian separation are then plotted as a function of position in the line profile, resulting in a "diagnostic diagram."

The diagnostic diagram for the Hα radial velocities of AE Aqr is shown in Figure 2. All measurements were made with Gaussian bandpasses characterized by $\sigma = 250$ km s^{-1}. We measured the velocities for Gaussian separations between 400 and 2000 km s^{-1} in steps of 400 km s^{-1}, and then determined the orbital elements for each value of the separation by fitting a sine curve to the velocities. The resulting values of K_{em} are shown in the top panel of the diagnostic diagram. The second panel shows σ_K/K, the fractional standard deviation of the measured value of K_{em}. The last two panels show γ, the sys-

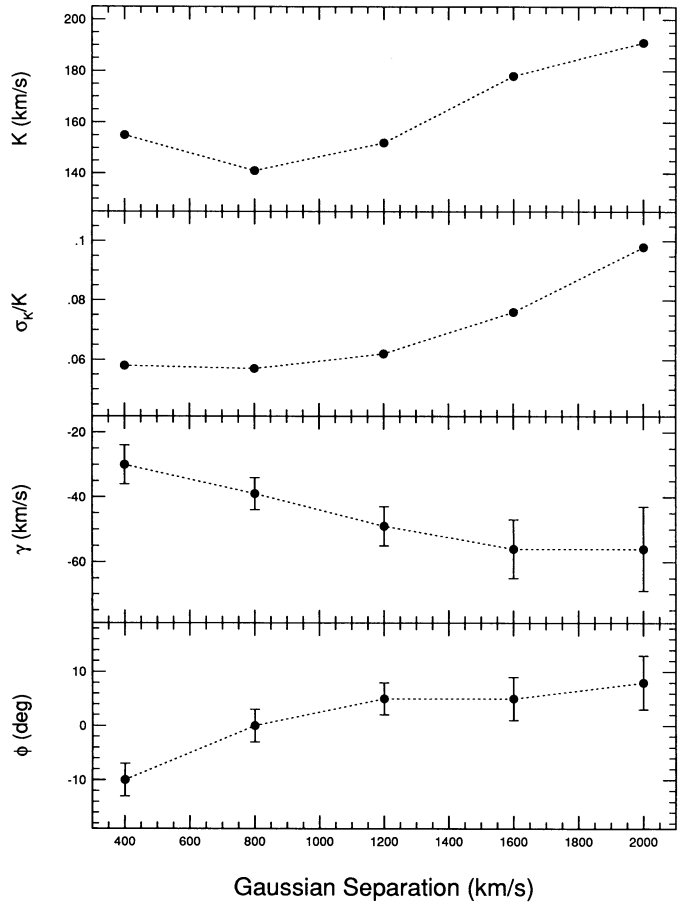

FIG. 2.—Diagnostic diagram for the Hα emission line in the spectrum of AE Aqr. The velocities of the emission line were measured at Gaussian separations between 400 and 2000 km s^{-1} in steps of 400 km s^{-1}. The orbital elements for each value of the Gaussian separation were determined by fitting a sine curve to the velocities. The resulting values of K_K are shown in the top panel of the diagnostic diagram. The second panel shows σ_K/K, the fractional standard deviation of the measured value of K_K. The last two panels show γ, the systemic velocity, and ϕ, the shift in the phase of the Hα orbit with respect to a fiducial orbit that is precisely 180° out of phase with the orbit of the K5 V star as determined by Feldt & Chincarini (1980).

temic velocity, and ϕ, the shift in the phase of the Hα orbit with respect to a fiducial orbit that is precisely 180° out of phase with the orbit of the K5 V star as determined by Feldt & Chincarini (1980). The diagnostic diagram for σ_K/K hits a shallow minimum at a Gaussian separation of 800 km s^{-1}, and the value of ϕ begins to flatten at a velocity near 1000 km s^{-1}. It appears that a good choice for the Gaussian separation is 800 km s^{-1}, and we will adopt this separation for the rest of our work on AE Aqr.

Hα radial velocities resulting from this separation are listed in Table 2. To optimize the emission-line orbital elements of AE Aqr, we combined the velocities in Table 2 with the velocities given by Joy (1954) and fitted an elliptical orbit by least squares. The eccentricity of the orbit was zero to within the measurement error, and, therefore, we refitted the velocities with a circular orbit:

$$V(t) = \gamma - K_{em} \sin\left[\frac{2\pi(t - T_0)}{P}\right], \quad (2)$$

TABLE 2

EMISSION-LINE RADIAL VELOCITIES OF AE AQUARII

HJD 2,400,000+	Velocity (km s^{-1})	HJD 2,400,000+	Velocity (km s^{-1})
46,314.629.....	72	46,316.789.....	−76
46,314.658.....	73	46,316.810.....	−111
46,314.689.....	−50	46,317.724.....	−203
46,314.742.....	−69	46,317.746.....	−162
46,314.766.....	−126	46,317.770.....	−109
46,314.791.....	−145	46,317.792.....	−101
46,314.814.....	−168	46,332.693.....	89
46,314.839.....	−163	46,333.608.....	−17
46,314.866.....	−114	46,333.631.....	−107
46,315.621.....	−153	46,333.658.....	−107
46,315.645.....	−171	46,333.682.....	−128
46,315.669.....	−160	46,333.706.....	−176
46,315.693.....	−121	46,334.653.....	−103
46,315.716.....	−75	46,334.682.....	−54
46,315.740.....	−27	46,334.710.....	0
46,315.766.....	25	46,335.613.....	146
46,315.789.....	70	46,335.637.....	133
46,315.814.....	84	46,335.660.....	91
46,315.838.....	76	46,335.683.....	42
46,315.862.....	125	46,341.662.....	−33
46,316.765.....	13	46,341.686.....	40

where T_0 is the time of inferior spectroscopic conjunction of the K5 V star. The resulting ephemeris for the emission-line orbit is

$$T_0 = \mathrm{JD}_\odot\, 2{,}439{,}030.830(\pm 3) + 0.4116580(\pm 2)E\,, \quad (3)$$

and the semiamplitude of the orbit is $K_{em} = 132 \pm 6$ km s^{-1}. Figure 3 shows the fit of the orbit to all the data.

The orbital solution described in the previous paragraph gives the best values for the orbital period and the time of spectroscopic conjunction because it uses data from the longest interval of time. It is the solution we outlined in an earlier report on AE Aqr (Robinson, Shafter, & Balachandran 1990). However, since the solution uses emission-line velocities

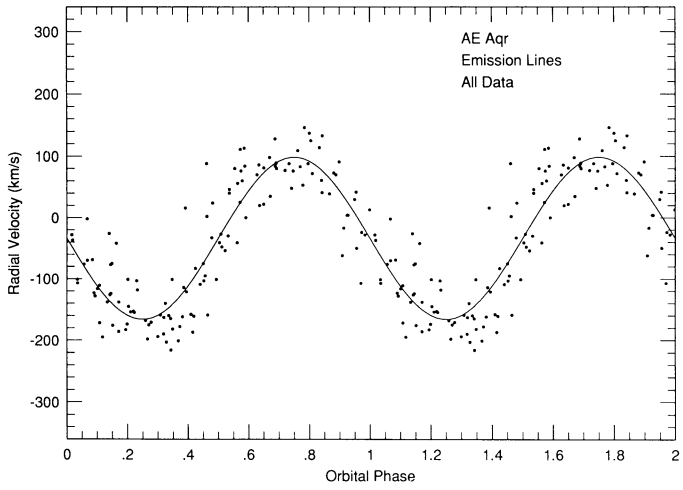

FIG. 3.—Emission-line orbit of AE Aqr. The emission-line velocities obtained by Joy (1954) and our new velocities obtained at McDonald Observatory in 1985 September and October have been folded at the best-fitting orbital period, 0.4116580 days, and plotted as a function of orbital phase. The solid line is the radial velocity curve resulting from fitting a circular orbit to the data.

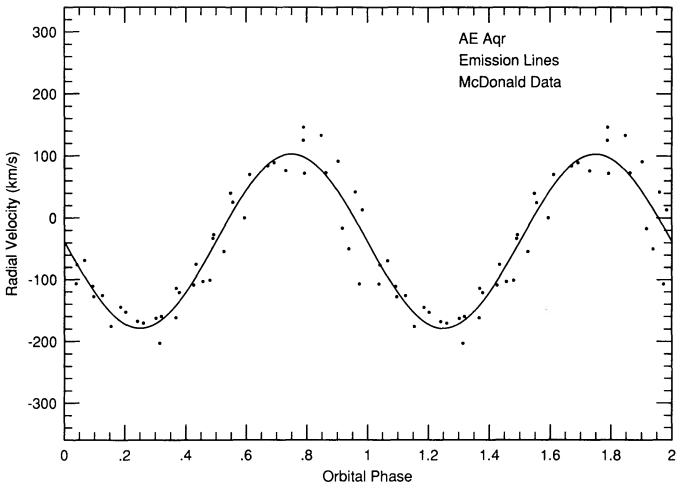

FIG. 4.—Emission-line orbit of AE Aqr; Similar to Fig. 3, but only the new velocities obtained at McDonald Observatory in 1985 September and October are shown. The solid line is the radial velocity curve resulting from fitting a circular orbit to just the McDonald data.

obtained by Joy (1954), which have potentially large biases, the solution does not give a reliable amplitude for the radial velocity variations. To determine the amplitude of the emission-line orbit, we refitted the orbit using just the new McDonald velocities, forcing the new fit to have the orbital period determined using Joy's velocities. Once again, a circular orbit is a good fit to the data. The amplitude of the radial velocity variation is $K_{em} = 141 \pm 8$ km s^{-1}, and the systemic velocity is $\gamma = -39 \pm 5$ km s^{-1}; Figure 4 shows the fit of the orbit to just the McDonald data.

The orbital elements are summarized in Table 3, where the orbital period and time of conjunction are derived from a fit to all the emission-line velocities, and the amplitude and systemic velocity are derived from just the McDonald velocities. The errors are the standard deviations determined during the least-squares fits and, as the diagnostic diagram makes clear, are certainly underestimates of the true errors.

4. PULSE-TIMING ORBIT

The normal procedure for measuring the times of arrival of the 33.08 s pulses would be to fit a sine curve with a period of 33.08 s to successive segments of the light curve. The mean time of arrival of the pulses in a segment would be given by the time of a peak of the sine curve near the center of the segment. Several factors forced us to modify this simple procedure. Since the 33.08 s periodicity has two nearly equal peaks in each pulse, its light curve is nearly a sine curve with a period of 16.5 s. Most of the timing information is contained in the 16.5 s first harmonic of the periodicity, not in the 33.08 s fundamental. This is shown clearly in the power spectra published by Patterson (1979), in which the power at 16.5 s is usually stronger than the power at 33.08 s. In consequence, the correct sine curve to fit to the light curve is one with a 16.5 s period, not a 33.08 s period. The ephemeris for the 16.5 s period does not distinguish which of a pair of successive pulse peaks corresponds to the peak of the 33.08 s period, but this information is irrelevant to the measurement of the pulse-timing orbit.

The unusual flares in the light curve of AE Aqr also complicate measurement of the pulse arrival times. Between the large flares, the light curve of AE Aqr is devoid of quasi-periodic oscillations and almost devoid of flickering, so that the 16.5 s periodicity is uncontaminated and easily measured. During the flares, however, random flickering and quasi-periodic oscillations appear. The pulses can be obscured by the random flickering or, worse, can be drowned out and effectively replaced by the quasi-periodic oscillations, so that the measured times of arrival are spurious. To avoid these problems, we did not use any segments of the light curves in which AE Aqr was obviously flaring. Also, we discarded any timing for which the formal standard deviation was greater than 3.5 s. With a standard deviation this large, the interval included within $\pm 2\,\sigma$ covers nearly an entire 16.5 s cycle, and the pulse timing is unreliable.

We extracted the times of arrival of the 16.5 s pulses by dividing the nonflare portions of the light curves into segments no more than 30 minutes long. To eliminate ringing and spectral leakage, the ends of the segments were tapered with a cosine bell data window. We then fitted a sine curve with a variable amplitude but a fixed period of 16.53838 s to each segment by least squares. The results are given in Table 4, in which the first column lists the barycentric Julian ephemeris dates (BJED) of maxima in brightness of the fitted sine curve and the second column the internal standard deviation of the fit in seconds.

Construction of a pulse-timing orbit for the 16.5 s pulses is an iterative process. Adopting a preliminary linear ephemeris for the times of arrival of the pulsations, we calculated the observed minus calculated ($O-C$) times of their arrival. We then derived a preliminary orbit for the pulses by folding the ($O-C$) times on the orbital period. Since the most accurate value of the orbital period is the value derived from the emission-line orbit, we used the emission-line orbital period throughout the analysis of the pulse orbit. Specifically, we adopted the following orbital ephemeris, in which the orbital period is the emission-line period and T_0 is arbitrary:

$$T_0 = \mathrm{JD}_\odot\, 2{,}445{,}172.000 + 0.4116580E\,. \qquad (4)$$

TABLE 3

ORBITAL ELEMENTS OF AE AQUARII (CIRCULAR ORBITS)

Orbital Element	Absorption[a] Lines	Emission Lines	Pulse Timings
Period (days)	0.4116579	0.4116580 ± 2	...[b]
T_0 (JD$_\odot$)[c]	2,439,030.827 ± 3	2,439,030.830 ± 3	2,445,172.284 ± 3
K (km s^{-1})	160 ± 1	141 ± 8	122 ± 4
γ (km s^{-1})	−64 ± 10	−39 ± 5	...

[a] Absorption-line elements from Feldt & Chincarini 1980.
[b] Adopted from the spectroscopic orbit.
[c] Time of spectroscopic conjunction, K star toward observer.

TABLE 4

TIMES OF PULSE MAXIMA OF THE 16 SECOND PULSES

BJED 2,445,000.0+	σ (s)	BJED 2,445,000.0+	σ (s)	BJED 2,445,000.0+	σ (s)
172.926270.....	1.14	258.655595.....	1.31	586.795626.....	1.08
173.825365.....	1.10	258.675126.....	1.43	586.816492.....	0.33
175.871243.....	1.89	260.571832.....	0.98	586.837367.....	0.33
175.893048.....	2.36	260.592511.....	3.33	587.627127.....	0.24
175.899759.....	0.60	528.717919.....	1.39	587.648582.....	0.16
175.938250.....	0.71	528.734036.....	1.35	587.670580.....	0.16
201.808145.....	1.27	528.753741.....	2.35	587.689716.....	1.09
201.840702.....	0.38	528.767136.....	1.58	587.752489.....	1.32
204.787960.....	0.92	528.780934.....	1.19	587.837274.....	0.73
204.806731.....	0.91	528.796052.....	1.53	588.629353.....	0.60
254.586480.....	0.62	528.816912.....	2.24	588.648311.....	0.59
256.578341.....	1.64	528.847918.....	2.09	588.683908.....	1.48
256.598442.....	0.98	528.868197.....	0.34	588.699986.....	1.44
256.617593.....	1.15	528.889623.....	0.42	588.716242.....	0.69
256.637304.....	0.79	528.907992.....	0.28	588.731577.....	0.60
256.657033.....	0.97	530.811284.....	0.35	589.662660.....	0.71
256.676555.....	0.95	530.837126.....	0.25	589.682745.....	0.62
257.633402.....	1.80	530.861247.....	2.04	589.764504.....	0.85
257.650244.....	1.54	530.874068.....	2.67	589.800643.....	0.52
258.578241.....	1.44	586.700264.....	0.35	589.819204.....	1.10
258.597761.....	1.09	586.716548.....	0.36	589.837956.....	1.04
258.617107.....	1.41	586.750419.....	0.32		
258.636063.....	1.09	586.761928.....	1.17		

At this stage one has a preliminary pulse orbit. The period of the 16.5 s pulses was then optimized by minimizing the scatter in the $(O-C)$ diagram about a circular pulse orbit. The resulting ephemeris for the 16.5 s pulses is

$$T_{\max} = \text{BJED } 2{,}445{,}171.999844(\pm 1) + 0.000191416425(\pm 1)E\,. \quad (5)$$

The period in this ephemeris differs from the ephemeris derived by Patterson (1979) because he used heliocentric times, while we have used barycentric times in our pulse measurements. Except for this difference, our period for the 16.5 s pulses is the same as Patterson's and the 16.5 s period is constant to within the errors of measurement.

The final orbital elements were derived by fitting a pulse orbit to the improved $(O-C)$ diagram using standard weighted least-squares methods. The best-fitting orbit had an eccentricity in the range of 0.2–0.3, but the standard deviation of this value was large and the true eccentricity could be nearly zero. Since both the absorption-line and the emission-line radial velocities are well fitted by circular orbits, and since there are good theoretical reasons why the orbit of AE Aqr cannot differ too greatly from a circular orbit, the eccentricity of the pulse orbit cannot represent the true orbital motion of the white dwarf and must be spurious. We chose, therefore, to fit a circular orbit to the $(O-C)$ diagram. As the pulse period had already been optimized against a circular orbit, no further improvement in the pulse period was necessary.

The $(O-C)$ diagram for the pulse-timing orbit is shown in Figure 5. The orbital phases and the pulse time delays in Figure 5 were calculated from equations (4) and (5). The solid line is the best-fitting circular orbit. The radius of the orbit is 2.30 ± 0.07 s, which is equivalent to $K_{\text{pulse}} = 122 \pm 4$ km s^{-1}. Our result agrees well with the radius determined by Patterson (1979), 2.40 ± 0.09 s. The revised value of T_0 is $\text{JD}_\odot$ 2,445,172.284 $\pm$ 0.003, where T_0 is now the time of superior conjunction of the pulse-timing orbit.

5. DISCUSSION

5.1. *Reprocessing of the* 33.08 s *Pulses*

Table 3 summarizes the orbital elements determined from the absorption-line and emission-line velocities, and from the pulse timings. The times of spectroscopic conjunction of the emission-line and absorption-line orbits are the same to within

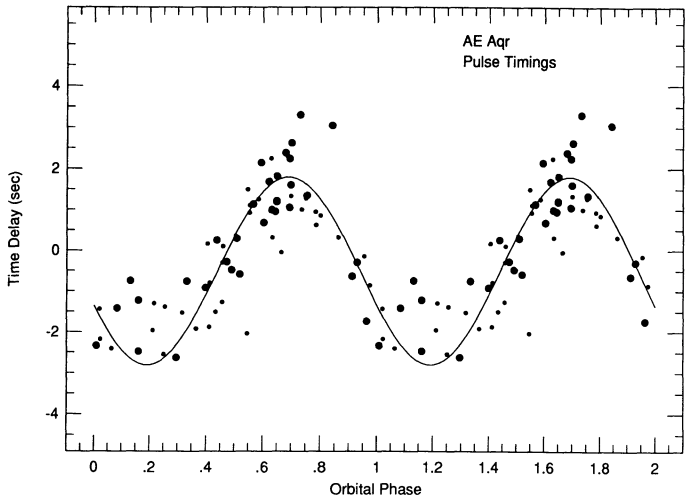

FIG. 5.—Pulse-timing orbit of AE Aqr. The figure shows the $(O-C)$ diagram for the pulse timings of the 16.5 s period in the light curve based on a test period of 0.00019146425 days for the periodicity. The $(O-C)$ diagram has been folded on the orbital period of AE Aqr to give the pulse-timing orbit of the white dwarf. The solid line is the best-fitting circular orbit and yields a semiamplitude of 2.30 ± 0.07 s.

the measurement error; the shift in orbital phase is $\Delta\phi = 3° \pm 4°$. The phase shift between the pulse-timing orbit and the absorption-line orbit is large, however. To find the phase shift, it is necessary to advance the time of spectroscopic conjunction of the absorption-line orbit to the same epoch as the pulse-timing orbit by adding an integral number of orbital periods. The result is $T_0 = \mathrm{JD}_\odot$ 2,445,172.353. The time of conjunction of the absorption-line orbit now differs from the time of conjunction of the pulse-timing orbit by 0.073 days, or by $60° \pm 3°$ in orbital phase. The pulse-timing orbit reaches conjunction before the absorption-line orbit. Our result differs substantially from that of Patterson (1979), who found that the phase shift of the pulse-timing orbit was small and consistent with no phase shift at all. The difference in the two results is due entirely to the improvement in the orbital period. Patterson was forced to calculate the spectroscopic orbital phase by extrapolating the orbital ephemeris determined by Chincarini & Walker (1981b) from data taken nearly 20 years earlier. We have recalculated the phase shift for Patterson's pulse-timing orbit using the improved orbital period, and find $\Delta\phi = 64°$, in close agreement with the phase shift for our data.

The large phase shift demonstrates that the pulse orbit is distorted and cannot be used to determine reliable orbital elements. The most obvious physical mechanism for producing the distortion is scattering or reprocessing of the pulses from the white dwarf by other parts of the binary system, so that the observed pulse is a sum of the direct pulse and a reprocessed pulse. Reprocessing is an especially attractive mechanism because it has been successful in explaining amplitude and phase shifts in other DQ Herculis stars and in pulsating X-ray sources (e.g., Middleditch & Nelson 1975; Warner 1986), and it can easily reproduce the amplitude and phase shift of the pulse-timing orbit in AE Aqr. The problem of determining the precise location of the reprocessing region in AE Aqr is, unfortunately, poorly constrained, since neither the relative amplitudes nor the relative phases of the direct and the reprocessed pulses are known. That the problem does have a solution is demonstrated by assuming that the direct pulse does not contribute in the observed pulses in the optical region of the spectrum. The pulse orbit would then describe the motion of the reprocessing region, and the projected position of the region is uniquely determined to be at 2.3 light seconds from the center of mass of the binary, at an angle of 60° preceding the white dwarf. The geometry for this solution is shown in Figure 6.

The location of the reprocessing region shown in Figure 6 is peculiar and almost certainly not precisely correct, because it lies outside the Roche lobe of the white dwarf. Large amounts of material that could serve as a reprocessing site should not be found there. We interpret this peculiar location as evidence that the direct pulse does contribute to the observed pulse, and that the location of the reprocessing region will need to be revised when data on the relative contributions of the direct and reprocessed pulses become available. We have calculated some numerical examples that include a contribution from the direct pulse, and these examples suggest that the location shown in Figure 6 is, nevertheless, likely to be qualitatively correct. We believe, therefore, that Figure 6 is roughly correct, but that the reprocessing region is closer to the white dwarf, so that it lies inside the Roche lobe.

We know of no reason why an accretion disk should reprocess pulses more efficiently at this location than any other, but it is interesting to note that the location is similar to the location of the bright regions in the disks of RW Tri and SW UMa (Horne & Stiening 1985; Shafter et al. 1986). As we noted

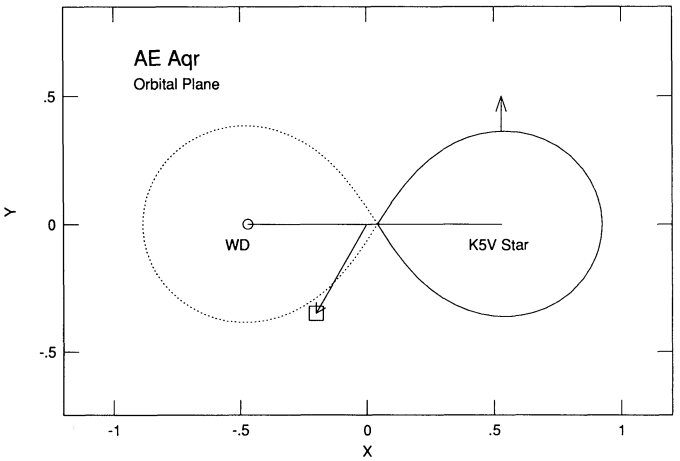

FIG. 6.—Geometry of AE Aqr in the orbital plane. The geometry is determined by the mass ratio, $q = M_{wd}/M_K = 1.13$, and by the assumption that the K5 V star fills its Roche lobe. The unit for the X and Y coordinates is the distance separating the centers of mass of the two stars. The Roche lobe around the white dwarf is shown by the dotted line, and the system is rotating counterclockwise. The approximate location of the reprocessing region is shown by the square. The vector from the center of mass of the binary system to the square is at an angle of 60° preceding the line to the white dwarf, and its length is given by the ratio of the projected size of the pulse-timing orbit, 2.30 s = 6.9×10^{10} cm, to the projected separation of the centers of mass of the two stars, 1.70×10^{11} cm.

in § 1 above, the evidence for an accretion disk in AE Aqr is poor, which raises another intriguing possibility for the source of the reprocessing material. Theoretical models of the trajectories of the stream of gas from the late-type stars in cataclysmic variables invariably show a large loop that extends to the boundary of the Roche lobe in roughly the direction of the reprocessing region shown in Figure 6 (e.g., Flannery 1975). The loop is present only if the transferred stream is not absorbed or deflected by the accretion disk on its first pass around the white dwarf. If the accretion disk in AE Aqr is sufficiently small or has a low enough density, the gas stream could survive long enough to make a loop and provide material to reprocess the pulses in the observed region.

The peculiar location of the reprocessing region suggests, nevertheless, that the reprocessing model should not be accepted without further tests. The model predicts that the periods of the direct and reprocessed pulses in AE Aqr should differ by an integral number of pulses per orbit (Warner 1986). Specifically, the rotation period of the white dwarf should be 33.046027 s. A light curve of AE Aqr at X-ray or far ultraviolet wavelengths should show this shorter period, although the light curve will have to be at least as long as the orbital period because the frequency difference will be comparable to the inverse of the orbital period.[3] Whether or not the model is

[3] After the manuscript of this paper was submitted, we received two papers reporting observations of AE Aqr at short wavelengths. Eracleous, Patterson, & Halpern (1991) reported that the 33 s pulses have the same period in the X-ray light curve as in the optical light curve. However, the X-ray data allow several alias periods, one of which is consistent with 33.046 s. Interestingly, the largest peak in the power spectrum of the X-ray light curves is at a period nearly equal to the mean of 33.046 and 33.0767 s. De Jager et al. (1991) report the detection of pulsed γ-rays from AE Aqr with a period equal to the optical period. They propose that the γ-rays are produced by inverse Compton scattering of soft photons from the disk or secondary star off hot electrons from the white dwarf. It is not clear what γ-ray pulse period the reprocessing model predicts under these conditions.

correct, however, our basic conclusion is unchanged: the pulse-timing orbit represents the true orbit of the white dwarf poorly.

5.2. *Reliability of the Emission-Line Orbit*

In contrast, the emission-line orbit passes the two primary tests for reliability: It is circular, and it is 180° out of phase with the absorption-line orbit to within measurement errors. Furthermore, the amplitude of the radial velocity variation appears to be insensitive to measurement technique. Although Joy (1954) used different equipment, different emission lines, and a different measurement technique, his measurements yield $K_{em} = 135 \pm 5$ km s^{-1}, in close agreement with our result (see Chincarini & Walker 1981b). The γ velocity of the emission-line orbit does not agree well with the γ velocity of the absorption-line orbit, but this is not unexpected. The γ velocity determined by the double-Gaussian method is sensitive to errors in the measured slope of the continuum. As long as the continuum placement is always done in a consistent way, the errors do not propagate to the other orbital elements. Thus, there is no reason not to accept the emission-line orbit as a good representation of the orbit of the white dwarf, at least at the level of accuracy to which the orbit has been measured.

We conclude that AE Aqr belongs to a small but growing group of cataclysmic variables for which the emission-line orbit does indeed give reliable results. The group includes systems such as LB 1800 and AH Her, for which the emission-line orbits appear to be free of phase shifts and spurious eccentricities (Buckley et al. 1990; Horne, Wade, & Szkody 1986). It also includes systems such as SS Cyg. The emission-line radial velocity curve of SS Cyg must be distorted because it is shifted in phase, but the shift is small, $\Delta\phi = 10° \pm 2°$, and the eccentricity of the orbit is nearly zero (Hessman et al. 1984). Furthermore, the amplitude of the emission-line radial velocity curve is the same as the amplitude of the radial velocity curve of the broad Balmer absorption lines that appear in its spectrum during eruptions. Hessman et al. (1984) concluded that the small distortions of the emission-line radial velocity curve have not altered its amplitude significantly.

5.3. *Masses of the Stars in AE Aqr*

The discussion of the previous section shows that the emission-line orbit gives the best available estimate of the true orbital motion of the white dwarf in AE Aqr. Adopting the spectroscopic orbital elements, we find

$$M_K \sin^3 i = 0.54 \pm 0.05\ M_\odot\ , \quad (6)$$

$$M_{wd} \sin^3 i = 0.62 \pm 0.05\ M_\odot\ , \quad (7)$$

$$q = M_{wd}/M_K = 1.13 \pm 0.06\ , \quad (8)$$

$$a_K \sin i = (9.06 \pm 0.06) \times 10^{10}\ \text{cm}\ , \quad (9)$$

$$a_{wd} \sin i = (7.98 \pm 0.45) \times 10^{10}\ \text{cm}\ , \quad (10)$$

where a_K and a_{wd} are the semimajor axes of the K star and white dwarf orbits.

Figure 7 shows the range of permitted masses for the stars in AE Aqr. The region outlined in dots is bounded by the formal error on q, which limits q to the range $1.07 < q < 1.19$. The region is also bounded by the requirements that the mass of the white dwarf be less than 1.4 $M_\odot$ and that the orbital inclination be less than 90°.

AE Aqr does not eclipse (van Paradijs et al. 1989). Since the K5 V star must fill or nearly fill its Roche lobe to transfer mass

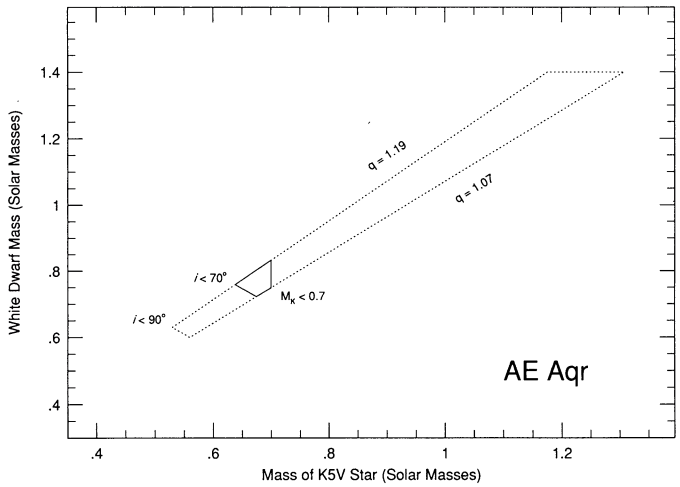

FIG. 7.—Range of permitted masses for the stars in AE Aqr. The region outlined by the dots is bounded by the formal standard deviation of the spectroscopic mass ratio, which limits q to the range $1.07 < q < 1.19$, and by the requirements that the orbital inclination must be less than 90° and the mass of the white dwarf must be less than 1.4 $M_\odot$. The solid lines outline the region bounded by the more stringent requirements that the orbital inclination must be less than 70° to avoid eclipses, and the mass of the K5 V star must be less than about 0.70 $M_\odot$.

to the white dwarf, the geometry of AE Aqr is fixed by its mass ratio, and the lack of eclipses places a more stringent limit on the orbital inclination. From the calculations by Chanan, Middleditch, & Nelson (1976), the orbital inclination must be less than 70° at the mass ratio of AE Aqr. This limit is shown as the solid line labeled "$i < 70°$" in Figure 7. Another lower limit to the mass of the white dwarf can be derived from its rotation period. To support a rotation period of 33 s, the white dwarf must have a mass greater than roughly 0.6 $M_\odot$ if it is a helium white dwarf, or 0.4 $M_\odot$ if it is an iron white dwarf (Hachisu 1986; Chanmugam, Rao, & Tohline 1987). These limits are consistent with, but do not improve, the limit placed by the lack of eclipses.

A rough upper limit to the mass of the late-type star can be determined from its spectral type. Chincarini & Walker (1981b) assigned a spectral type of K5 V to the late-type star from a careful examination of the line ratios in its spectrum. A main-sequence star with this spectral type has an absolute visual magnitude near 7.4 (Gliese 1982), which corresponds to a mass of about 0.70 $M_\odot$ (Lacy 1977). It is also possible to determine the spectral type of the late-type star from its photometric colors. The infrared colors should be used for the spectral typing instead of visual colors, because the infrared colors are less contaminated by light from the white dwarf and the accretion disk. According to Bailey (1981) the $V-K$ infrared color of AE Aqr corresponds to a spectral type of K6–K7. This spectral type yields a mass somewhat less than 0.70 $M_\odot$.

The spectral types of the late-type stars in cataclysmic variables can fail to yield accurate masses under two severe conditions. If the time scale for mass transfer is comparable to the thermal time scale, the late-type star is driven away from thermal equilibrium, and the relation between its surface temperature and its core luminosity will differ from the relation for main-sequence stars. This probably happens in cataclysmic variables with orbital periods less than about 90 minutes, and may happen at orbital periods between 3 and 4 hr, just above

the period gap (Rappaport, Verbunt, & Joss 1983; Spruit & Ritter 1983). The time scale for mass transfer in AE Aqr is, however, extremely long because of its low rate of mass transfer: $\tau \sim M/\dot{M} \sim 10^{10}$ yr. The later-type star should, therefore, be close to thermal equilibrium. The late-type star in a cataclysmic variable is irradiated by the white dwarf and the accretion disk. If the white dwarf and the accretion disk have a high enough luminosity, they can heat one face of the late-type star and alter its spectral type (Robinson, Zhang, & Stover 1986). In systems with high orbital inclinations such as AE Aqr, this effect will display itself as a spectral type that varies systematically with orbital phase. The spectral type of the late-type star in AE Aqr may, in fact, be varying with orbital phase, but the variation is probably due to the change in effective gravity near the inner Lagrangian points, not to heating (Crawford & Kraft 1956). Since the late-type star is neither far from thermal equilibrium nor strongly heated, it is reasonable to accept the various estimates of its spectral type and to adopt the highest of the masses determined from the spectral types, 0.70 $M_\odot$, as an upper limit to its mass. This limit is shown as the solid line labeled "$M_K < 0.7$" in Figure 7. This limit should not, however, be considered firm. Other physical mechanisms than those we have considered could conceivably be at work and could weaken the correlation between the spectral type and the mass of the lobe-filling star.

The allowable range of masses is shown by the region outlined by the solid line in Figure 7. If we ignore systematic errors, the masses of the stars in AE Aqr are confined to the ranges $0.64\ M_\odot < M_K < 0.70\ M_\odot$ and $0.72\ M_\odot < M_{wd} < 0.83\ M_\odot$, and the orbital inclination must lie in the range $63° < i < 70°$. If the spectral type of the late-type star is closer to K6–K7, the masses of the stars must be near their lower limits, and the orbital inclination must be close to 70°. We emphasize, however, that although the masses and inclination appear to be limited to narrow ranges, Figure 2 shows that systematic errors could be larger than the internal errors, and the permitted range of mass and inclinations could be larger than we have stated.

We thank S. Sawyer, B. P. Hine, and D. Gies for help in acquiring the data reported here. This work was supported in part by NSF grant AST87-04382.

REFERENCES

Bailey, J. 1981, MNRAS, 197, 31
Bastian, T. S., Dulk, G. A., & Chanmugam, G. 1988, ApJ, 324, 431
Bookbinder, J. A., & Lamb, D. Q. 1987, ApJ, 323, L131
Buckley, D. A. H., Sullivan, D. J., Remillard, R. A., Tuohy, I. R., & Clark, M. 1990, ApJ, 355, 617
Chanan, G. A., Middleditch, J., & Nelson, J. E. 1976, ApJ, 208, 512
Chanmugam, G., Rao, M., & Tohline, J. E. 1987, ApJ, 319, 188
Chincarini, G., & Walker, M. F. 1981a, ESO Sci. Preprint, No. 134
———. 1981b, A&A, 104, 24
Crawford, J. A., & Kraft, R. P. 1956, ApJ, 123, 44
de Jager, O. C., et al. 1991, private communication
Eracleous, M., Patterson, J., & Halpern, J. P. 1991, ApJ, 370, 330
Feldt, A. N., & Chincarini, G. 1980, PASP, 92, 528
Flannery, B. P. 1975, MNRAS, 170, 325
Gliese, W. 1982, in Landolt-Börnstein, Numerical Data and Functional Relationships in Science and Technology, N.S., Group VI, Vol. 2c, p. 147
Hachisu, I. 1986, ApJS, 61, 479
Henize, K. G. 1949, AJ, 54, 89
Hessman, F. V., Robinson, E. L., Nather, R. E., & Zhang, E.-H. 1984, ApJ, 286, 747
Horne, K., & Marsh, T. R. 1986, MNRAS, 218, 761
Horne, K., & Steining, R. 1985, MNRAS, 216, 933
Horne, K., Wade, R. A., & Szkody, P. 1986, MNRAS, 219, 791
Jameson, R. F., King, A. R., & Sherrington, M. R. 1980, MNRAS, 191, 559
Joy, A. H. 1954, ApJ, 120, 377
Lacy, C. H. 1977, ApJS, 34, 479
Lamb, D. Q., & Patterson, J. 1985, in Cataclysmic Variables and Low Mass X-Ray Binaries, ed. D. Q. Lamb & J. Patterson (Dordrecht: Reidel), 229
Lomb, N. R. 1976, Ap&SS, 39, 447
Middleditch, J., & Nelson, J. E. 1975, ApJ, 208, 567
Nather, R. E. 1973, Vistas Astr. 15, 91
Patterson, J. 1979, ApJ, 234, 978
Patterson, J., Beuermann, K., & Africano, J. 1988, BAAS, 20, 1099
Patterson, J., Branch, D., Chincarini, G., & Robinson, E. L. 1980, ApJ, 240 L133
Rappaport, S., Verbunt, F., & Joss, P. C. 1983, ApJ, 275, 713
Robinson, E. L., Shafter, A. W., & Balachandran, S. 1990, in Proc. 11th North American Workshop on CVs and LMXRBs, ed. C. W. Mauche (Cambridge: Cambridge Univ. Press), 219
Robinson, E. L., Zhang, E.-H., & Stover, R. J. 1986, ApJ, 305, 732
Scargle, J. D. 1982, ApJ, 263, 835
Shafter, A. W. 1985, in Cataclysmic Variables and Low Mass X-Ray Binaries, ed. D. Q. Lamb & J. Patterson (Dordrecht: Reidel), 355
Shafter, A. W., Szkody, P., & Thorstensen, J. R. 1986, ApJ, 308, 765
Spruit, H. C., & Ritter, H. 1983, A&A, 124, 267
Stover, R. J., Robinson, E. L., & Nather, R. E. 1981, ApJ, 248, 696
van Paradijs, J., Kraakman, H., & van Amerongen, S. 1989, A&AS, 79, 205
Vogt, S. S., Tull, R. G., & Kelton, P. 1978, Appl. Optics, 17, 574
Walker, M. F. 1965, S&T, 29, 23
Warner, B. 1986, MNRAS, 219, 347
Zinner, E. 1938, Astr. Nach., 265, 345